Mechanochemical synthesis and high-capacity performances of transition-metal borides as aqueous anode materials

WANG YaDong[1*], GUANG XianYong[2] & PAN Mu[1]

[1] *State Key Laboratory of Advanced Technology for Materials Synthesis and Processing, Wuhan University of Technology, Wuhan 430070, China;*

[2] *Department of Chemistry, Wuhan University, Wuhan 430072, China*

Transition-metal borides $MB_{0.5}$ (M = Co, Mo, V) were synthesized by high-speed mechanical ball-milling of the corresponding elemental metals and boron, and investigated as aqueous anode materials. The as-synthesized borides can achieve an excellent discharge capacity, about twice that of their parent transition metals. The metal boride electrodes also exhibit polarizations about 100–300 mV lower than those of their parent metals. The galvanostatic discharge curve of $CoB_{0.5}$ shows a single discharge voltage plateau as a result of simultaneous electro-oxidation of elemental cobalt and/or amorphous cobalt boride. Both $MoB_{0.5}$ and $VB_{0.5}$ show two well-defined voltage plateaus, corresponding to the electro-oxidation of the corresponding metal and boride. These results show that the coexisting transition metal and boride in the metal borides co-activate each other in the ball-milling process, thereby significantly enhancing their electrochemical performances.

Metal borides have received considerable attention recently because of their high specific capacities as anode materials in both alkaline and neutral electrolytes [1–8]. In our earlier work, crystalline VB_2 was found to deliver a very high discharge capacity of above 3100 mAh g^{-1} through a simultaneous 11-electron electrochemical oxidation; this is probably the highest specific capacity observed so far for aqueous anode materials [1]. The effective electro-activation of crystalline borides represented by VB_2 is attributed to at least two factors. One is the improved electronic conductivity of the boron component as a result of the alternating boron layers and transition metal (TM) layers in the MB_2 lattice. The other is the synergistic effects of boron and TM: electron donation from the TM atoms to the boron atoms weakens the bonds between the boron atoms, resulting in electrochemical activation of boron. Conversely, the activation of boron alleviates the passivation of the TM and leads

to TM activation. These activations ensure electro-oxidation of both TM and boron in the TM borides, resulting in the very high-capacity output of the borides.

To test the potential of other types of metal borides for high-capacity anode materials, we synthesized a series of $MB_{0.5}$ (M = Co, Mo, and V) by mechanical ball-milling and investigated their electrochemical properties as aqueous anodes. In this paper, we report the synthesis, polarization behaviors, and high-capacity performances of these $MB_{0.5}$ compounds. The mechanisms of electrochemical activation of the borides are also discussed.

1 Experimental

1.1 Preparation of $MB_{0.5}$

The $MB_{0.5}$ borides (M = Co, Mo, and V) were prepared by mechanical ball-milling a mixture of the elemental TM (Co, Mo, or V) and boron powders in a TM:boron atomic ratio of

1:0.5, using a high-energy-shaker ball-miller (QM-3A, Nanjing University Instrument Plant, China). The particle sizes of all the TM powders (Beijing Mountain Technical Development Center, China) were 200 mesh, and the purities were 99%. The particle size of the boron powder (Changsha Hengrui New Material Development Co. Ltd, China) was 325 mesh, with 95% purity. The ball-milling process was performed for 20 h under an argon atmosphere to prevent surface oxidation. The shaker speed was set at 1200 r/min. A B/C composite was synthesized in the same way, but with a weight ratio of boron to carbon of 2:3.

1.2   Materials characterizations

The as-synthesized TM borides were examined by powder X-ray diffraction (XRD) using a Shimadzu Lab XRD-6000 diffractometer with a Cu Kα source. The scan speed was set at 4° min^{-1} and the data were collected over a scattering angle range of $2\theta = 10°$–$80°$.

The thin-film electrodes were prepared by mixing 85% boride powders, 7% polytetrafluoroethylene (in a 60% emulsion), and 8% acetylene black into a paste, and then roll-pressing the paste into films of thickness 0.15 mm at a temperature of 40–60°C. The electrodes were finished by pressing the films onto stainless-steel mesh as a current collector.

Cyclic voltammetric (CV) measurements were performed in a three-electrode cell using a 3 mm × 3 mm boride film electrode as the working electrode, a large-area air electrode as the counter electrode, and Hg/HgO in the electrolyte as the reference electrode. The electrolyte was 6 mol L^{-1} KOH aqueous solution. CV was conducted using a CHI660a electrochemical workstation.

The discharge performances of the boride electrodes were evaluated by galvanostatic discharge experiments using laboratory cells similar to those used for CV, but with a 1 cm × 1 cm boride electrode as the anode, with a battery-testing system (NEWARE BTS-610).

2   Results and discussion

Figure 1 compares the XRD patterns of the ball-milled VB$_{0.5}$ samples with that of elemental vanadium. The as-prepared VB$_{0.5}$ shows well-resolved diffraction peaks of metallic vanadium and featureless bands at $2\theta = 35°$–$45°$, reflecting the presence of elemental vanadium and amorphous vanadium boride in the VB$_{0.5}$ sample. The XRD lines of CoB$_{0.5}$ and MoB$_{0.5}$ were in a similar pattern to that for VB$_{0.5}$.

To reveal the basic electrochemical behavior of the as-prepared MB$_{0.5}$ samples, CVs for CoB$_{0.5}$, MoB$_{0.5}$, and VB$_{0.5}$, were measured. As shown in Figure 2, all three electrodes show two obvious current peaks in the positive scan, indicating at least two-step anodic oxidations in these
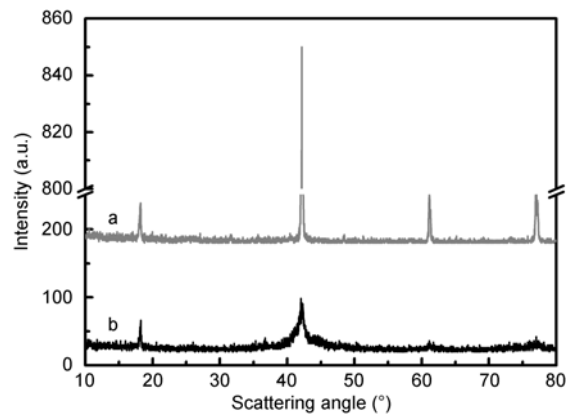

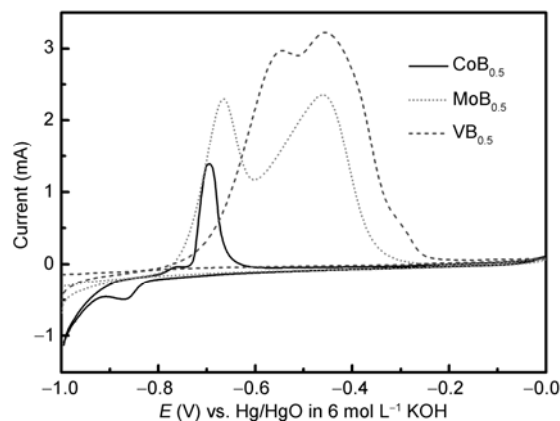**Figure 1**   XRD patterns of (a) V and (b) VB$_{0.5}$.

Figure 2   CVs of the MB$_{0.5}$ electrodes in a 6 mol L^{-1} KOH solution. Potential sweep rate was set at 0.05 mV s^{-1}.

samples. The two current peaks for CoB$_{0.5}$ are located at −0.77 and −0.70 V, respectively. A reductive current peak is also found at −0.86 V when the negative scan is imposed. The anodic peaks could originate from electro-oxidation of boron, cobalt, and the amorphous cobalt boride. In an alkaline electrolyte, the electro-oxidation of cobalt probably takes place as follows:

$$Co(OH)_2 + 2e^- \rightarrow Co + 2OH^- \qquad (1)$$
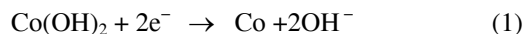
The standard equilibrium potential for this reaction is −0.73 V vs. SHE [9]. The calculated equilibrium potential for cobalt in 6 mol L^{-1} KOH is about −0.83 V vs. Hg/HgO when the pH is greater than 14. The onset potential for the two electro-oxidations of CoB$_{0.5}$ shown in Figure 2 are −0.79 and −0.74 V. The first one is more negative than the equilibrium potential shown in eq. (1), indicating that the first current peak could not arise from cobalt electro-oxidation. Since the equilibrium potential of boron (−1.79 V vs. SHE [9]) is more negative than the first onset potential, and boron is usually passivated in alkaline electrolytes, the first weak current peak could be attributed to the electro-oxidation of boron or amorphous cobalt boride. Consequently, the second strong anodic current peak should mainly or totally come from oxidation of cobalt (according

to the discharge curve). The cathodic current peak for $CoB_{0.5}$ should arise from electroreduction of $Co(OH)_2$, since borate, the product of boron oxidation, cannot be reduced at this potential, according to the standard reductive potential of borate [9].

The two anodic current peaks of the $MoB_{0.5}$ electrode are located at −0.67 and −0.46 V. The second current peak shows a large integrated area, suggesting a higher discharge specific capacity. The two anodic current peaks of the $VB_{0.5}$ electrode are located at −0.55 and −0.45 V. Unlike the CV of $CoB_{0.5}$, the two anodic current peaks for both $MoB_{0.5}$ and $VB_{0.5}$ overlap. Because the onset potentials of the current peaks for both $MoB_{0.5}$ and $VB_{0.5}$ are more positive than the equilibrium potential of their parent TM elements under the same conditions, it is difficult to determine the electro-oxidation reaction(s) producing the two current peaks simply from the CV curve.

Figure 3 compares the galvanostatic discharge curves of $CoB_{0.5}$, the B/C composite, and cobalt in 6 mol L^{-1} KOH solution. The current density for both $CoB_{0.5}$ and cobalt was set at 100 mA g^{-1}, and the current density for B/C was set at 50 mA g^{-1}. The $CoB_{0.5}$ electrode showed an open-circuit voltage of 1.06 V and a specific capacity of 245 mAh g^{-1} with a single discharge voltage plateau at about 0.75 V. The shape of the discharge curve of elemental cobalt is similar to that of $CoB_{0.5}$, but the discharge capacity, open-circuit voltage, and plateau voltage are much lower than those of $CoB_{0.5}$. The B/C composite electrode showed a voltage hump initially, followed by a voltage plateau at about 0.36 V at a discharge current density of 50 mA g^{-1}. Although the boron-based cells have discharge capacities of 300 mAh g^{-1} and much lower voltage plateaus than those of cobalt- and $CoB_{0.5}$-based cells, electro-activation of boron is clearly seen after ball-milling with conductive carbon, since elemental boron has no detectable discharge capacity under the same conditions. The activation of boron can be attributed to improved electronic conductivity as a result of combination with carbon. The appearance of a voltage hump at the

beginning of the discharge curve for the B/C composite is probably the result of surface passivation of boron; this was then alleviated by prolonged discharge. Comparison of the discharge curves shows that the $CoB_{0.5}$ electrode demonstrates considerable electrochemical mutual activation of cobalt and boron. Although the theoretical capacity, as shown in Table 1, is not achieved, the $CoB_{0.5}$ electrode exhibits a much higher capacity and lower polarization than elemental cobalt does.

Figure 4 shows the discharge curve of $MoB_{0.5}$. The open-circuit voltage is 0.94 V, and two voltage plateaus appear at ~0.7 and 0.5 V, in accordance with the two current peaks in the CV. The discharge capacity from the first voltage plateau is about 500 mAh g^{-1}, and the second one is about 850 mAh g^{-1}, which is in agreement with the electronic quantities measured from the area of the current peak in the CV. As shown in Table 1, the capacity discharged from either of the voltage plateaus is larger than the theoretical capacity of boron, suggesting that neither of the voltage plateaus can solely originate from electro-oxidation of boron in $MoB_{0.5}$. It is well known that molybdenum can be oxidized to multivalent molybdenum cations with valences from +3 to +6 by 3–6-electrons oxidations. Earlier work [10] reported that a mixture of Mo(VI) and Mo(V) is blue, and Mo(V) tends to disproportionate in solution. During the discharge process, the color of the electrolyte

Table 1 Capacity analysis of $MB_{0.5}$[a]

$TMB_{0.5}$	Theoretical specific capacity (mAh g^{-1})			Experimental specific capacity (mAh g^{-1})		
	Total	From TM	From B	Total	1st voltage plateau	2nd voltage plateau
$CoB_{0.5}$	1457	833	624	245	~0	~245
$MoB_{0.5}$	1983	1587	396	1388	~500	~850
$VB_{0.5}$	3089	2376	713	2158	~1430	~720

a) The theoretical specific capacity of $CoB_{0.5}$, $MoB_{0.5}$ and $VB_{0.5}$ is calculated based on Co, Mo, V and B, which are oxidized to 2^+, 6^+, 5^+ and 3^+, respectively.
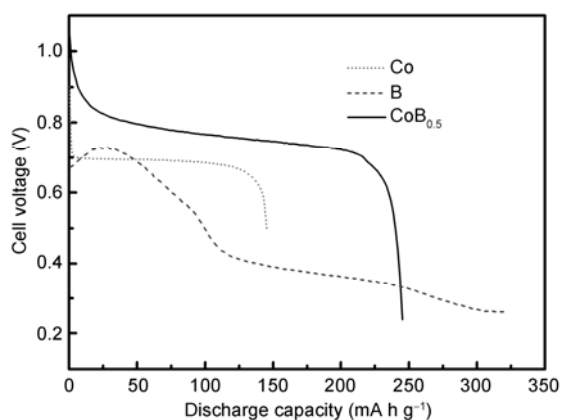

Figure 3 Galvanostatic discharge curves of cells using Co, B/C composite, and $CoB_{0.5}$ anodes. The current densities are 50 mA g^{-1} for B/C, and 100 mA g^{-1} for Co and $CoB_{0.5}$.

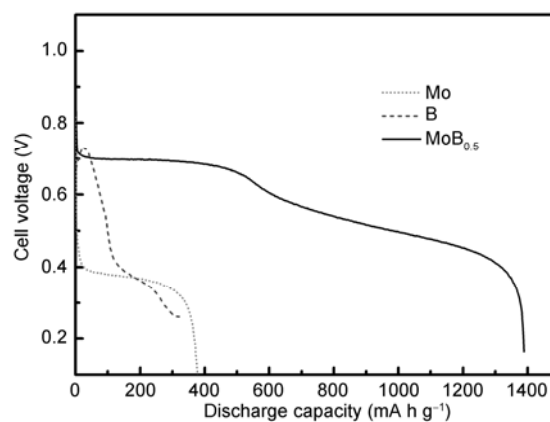**Figure 4** Galvanostatic discharge curves of cells using Mo, B/C composite, and $MoB_{0.5}$. The current densities are 50 mA g^{-1} for B/C, and 100 mA g^{-1} for Mo and $MoB_{0.5}$.

changed to blue and then became colorless, suggesting that most of the molybdenum in $MoB_{0.5}$ is electro-oxidized to Mo^{5+} rather than to Mo^{6+}. The theoretical oxidation capacity of molybdenum in $MoB_{0.5}$ to Mo(V) is 1322 mAh g^{-1}, which is lower than the experimental discharge capacity of $MoB_{0.5}$. This suggests simultaneous activation of both molybdenum and boron in $MoB_{0.5}$. The two voltage plateaus of the $MoB_{0.5}$ electrode should therefore come from the electro-oxidation of molybdenum and amorphous MoB_x, although it is difficult to determine the detailed reaction sequence. Compared with the experimental specific capacity of 370 mAh g^{-1} and the voltage plateau of 0.35 V for elemental molybdenum, $MoB_{0.5}$ shows a much higher discharge capacity and much lower polarization.

The discharge curve of $VB_{0.5}$ in Figure 5 shows an open-circuit voltage of 0.97 V and two clear voltage plateaus at 0.7 and 0.5 V; this is in agreement with the CV results. According to the capacity analysis in Table 1, the experimental capacity is higher than the theoretical capacity if only boron is oxidized in $VB_{0.5}$. This demonstrates that both boron and vanadium are electrochemically activated in the $VB_{0.5}$ structure. Comparison of the discharge curves of elemental vanadium and $VB_{0.5}$ shows that $VB_{0.5}$ has a much lower polarization and higher discharge capacity than vanadium does; this is similar to the cases of $CoB_{0.5}$ and $MoB_{0.5}$.

3 Conclusions

The $CoB_{0.5}$, $MoB_{0.5}$, and $VB_{0.5}$ synthesized in this work show simultaneous electro-activation of both the TM and boron. The as-prepared borides have discharge capacities almost twice those of their parent TMs, and they have much lower polarizations. $CoB_{0.5}$ shows one merged discharge voltage plateau originating from the electro-oxidation of cobalt and/or amorphous cobalt boride. Both $MoB_{0.5}$ and $VB_{0.5}$ show two discharge voltage plateaus originating from electro-oxidation of the TM and boride.
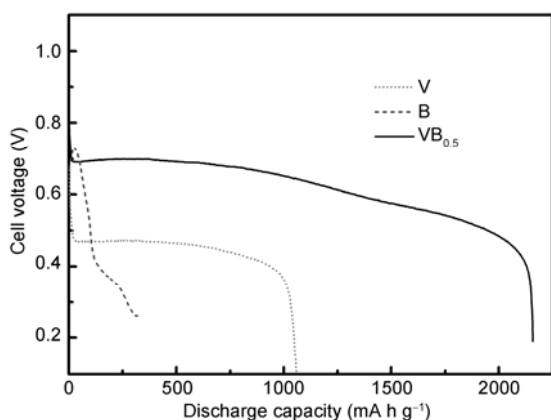
Figure 5 Galvanostatic discharge curves of the cells using V, B/C composite, and $VB_{0.5}$. The current densities are 50 mA g^{-1} for B/C, and 100 mA g^{-1} for V and $VB_{0.5}$.

1   Wang Y, Ai X, Cao Y, et al. Exceptional electrochemical activities of amorphous Fe-B and Co-B alloy pow-ders used as high capacity anode materials. Electrochem Commun, 2004, 6: 780–784

2   Wang Y, Guang X, Cao Y, et al. Electrooxidation and dischargeability of transition-metal borides as possible anodic materials in neutral aqueous electrolytes. J Appl Electrohcem, 2009, 3: 1039–1044

3   Wang Y, Guang X, Cao Y, et al. Mechanochemical synthesis and electrochemical characterization of VBx as high capacity anode materials for air batteries. J Alloy Compd, 2010, 501: L12–L14

4   Licht S, Wu H, Yu X, et al. Novel alkaline redox couple: Chemistry of the Fe^{6+}/B^{2-} super-iron boride battery. Chem Commun, 2007, 26: 2753–2755

5   Licht S, Ghosh S, Wang B, et al. Nanoparticle facilitated charge transfer and voltage of a high capacity VB2 anode. Electrochem Solid State Lett, 2011, 14: A83–A85

6   Yu X, Licht S. A novel high capacity, environmentally benign energy storage system: Super-iron boride battery. J Power Sources, 2008, 179: 407–411

7   Licht S, Yu X, Wang Y, et al. The super-iron boride battery. J Electrochem Soc, 2008, 155: A297–A303

8   Bard A J, Parsons R, Jordan J. Standard Potentials in Aqueous Solution. New York: Marcel Dekker, 1985. 799

9   Milazzo G, Caroli S, Sharma V K. Tables of Standard Electrode Potentials. New York: John Wiley & Sons, 1978. 115

10 Shen P W, Che Y X, Luo Y J, et al. Inorganic Chemistry Series. Vol. 8. Xi'an: Science Press, 1984. 470